Study on Mounting Position of IMU for Better Accuracy of ZUPT-Aided Pedestrian Inertial Navigation

Yusheng Wang, Sina Askari, and Andrei M. Shkel
MicroSystems Laboratory, University of California, Irvine, CA, USA
Email: {yushengw, askaris, andrei.shkel}@uci.edu

***Abstract*—We present a study on the effect of mounting position of IMU to a foot on the navigation accuracy of ZUPT-aided pedestrian inertial navigation. In this study, we compared two IMU mounting positions, forefoot and heel, in terms of the length of the stance phase, velocity uncertainty, and the shock level during the stance phase. Circular Error Probable (CEP) of localization was experimentally demonstrated to be reduced by about 50%, when mounting the IMU on the forefoot rather than behind the heel. The conclusion was demonstrated by investigating different walking paces, types of floors (hard floor, grass lawn, and sand), trajectories (upstairs and downstairs), and gait patterns produced by different persons. To the best of our knowledge, this study is the first attempt to investigate the velocity uncertainty during the stance phase in pedestrian navigation, a critical characteristic of ZUPT-aided algorithms.**

***Index Terms*—pedestrian inertial navigation; IMU mounting position; ZUPT; velocity uncertainty; stance phase**

I. Introduction

The rapid development of Micro-Electro-Mechanical Systems (MEMS)-based Inertial Measurement Units (IMUs) resulted in better performance, smaller size, and lower cost of the navigation system, and therefore made possible self-contained pedestrian inertial navigation [1]. Without proper compensation algorithms, however, the navigation error accumulates approximately proportional to the time cubed and will exceed a meter of error within only a few seconds of navigation for consumer grade IMUs [2]. Zero-Velocity-Update (ZUPT) algorithm [3] is one of the commonly used compensation mechanisms for self-contained pedestrian inertial navigation, which does not require any other sensor input besides IMU.

ZUPT algorithm takes advantage of the stationary state of the foot during the stance phase and feeds the zero-velocity information into Kalman Filter (KF) to compensate for IMU errors. It has been demonstrated that ZUPT algorithm can greatly reduce the position error of navigation and also suppress it from propagating as t^3 to $t^{1.5}$ [4]. Even with such algorithmic improvements, the final navigation error still remains dependent on many parameters during navigation, such as Angle Random Walk (ARW) of gyroscopes, Velocity Random Walk (VRW) of accelerometers, sampling frequency of IMUs, shock level during walking, percentage of the stance phase during the whole gait cycle, and velocity uncertainty during the stance phase [5]. The first three of the previously mentioned parameters are determined by the performance of IMU. However, the other parameters, such as the shock level, the duration of the stance phase, and the velocity uncertainty during the stance phase, are related to gait patterns and mounting positions of IMUs. Two commonly used mounting positions of IMUs are above the forefoot [6] and behind the heel [7]. To the best of our knowledge, no systematic study has been conducted to date on how the two mounting positions affect the navigation accuracy. Furthermore, all the listed parameters influencing the accuracy of navigation are relatively easy to measure, except the velocity uncertainty during the stance phase. Some typical velocity uncertainty values were assumed varying from 0.001m/s to 0.1m/s [3], [8], [9], but no verification of the assumptions was provided. This paper intends to fill these gaps.

Fig. 1. A setup of foot-mounted IMUs. Two identical near-tactical grade VN-200 IMUs are rigidly mounted on the forefoot and behind the heel of the boot by 3D-printed fixtures, respectively.

In this paper, we present a study on preferential IMU mounting position. The approach used in this study was as follows: two identical IMUs were first attached to the forefoot and the heel of the boot to collect data during walking, Fig. 1. Then, collected IMU data were averaged to extract the length of the stance phase, shock level, maximum acceleration

This work was performed under the following financial assistance award: 70NANB17H192 from U.S. Department of Commerce, National Institute of Standards and Technology (NIST).

978-1-5386-7828-2/19/$31.00 ©2019 IEEE

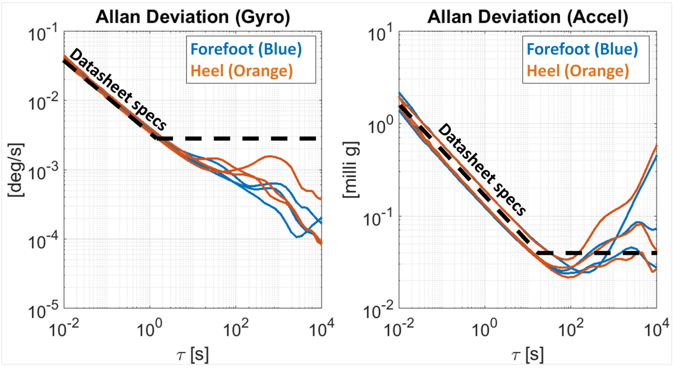

Fig. 2. Noise characteristics of the IMUs used in this study.

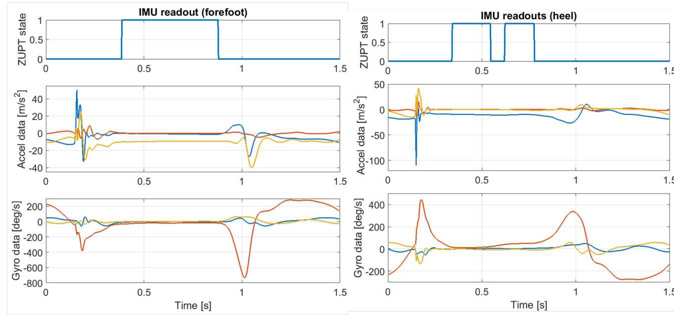

Fig. 3. Comparison of averaged IMU data and ZUPT states from IMUs mounted on the forefoot and behind the heel. Stance phase is identified when ZUPT state is equal to 1.

and angular rate of the forefoot and the heel during walking. Next, a technique to extract the velocity uncertainty during the stance phase was developed to evaluate the two IMU mounting positions. The same analysis was conducted with different floor types and step paces, trajectories, and persons, and then the conclusion on the IMU mounting positions was drawn in all cases. Finally, navigation experiments were conducted, supporting fidelity of the conclusions.

II. Data Collection

Two identical near-tactical grade IMUs (VectorNav VN-200 IMU) were rigidly mounted above the forefoot and behind the heel of the boot, respectively, to collect data of the motion of the forefoot and the heel simultaneously. Noise characteristics of the two IMUs were first estimated by Allan Deviation analysis and compared to the datasheet [10]. The results are presented in Fig. 2, showing that the two IMUs had the same noise level, eliminating some possible discrepancies in experiment due to IMU characteristics.

With IMUs mounted on the forefoot and behind the heel of the boot, experiments were conducted by walking on different floor types, with different paces and by different persons, assuring validity of conclusions. For each experiment, a trajectory with 600 strides (1200 steps) was recorded. The walking pace was fixed with the help of a metronome for a better averaging result during post-processing. Floor types, such as hard floor, grass lawn, and sand floor, were tested. Walking paces ranged from 84 to 112 steps per minute. Trajectories, such as walking upstairs and downstairs, were also investigated. Four different walking patterns by four persons were tested in this study. IMU readouts were collected during walking and then analyzed in post-processing.

III. Data Processing

Collected IMU data from the forefoot and the heel were processed to compare the two mounting positions. IMU data were first averaged to reduce the noise level and extract parameters, such as length of the stance phase and the shock level during walking. Next, a method to extract the velocity uncertainty during the stance phase was developed and applied to the IMU data to evaluate the two IMU mounting positions.

A. Data Averaging

In this process, IMU data of 600 gait cycles were averaged. The main purpose of averaging was to remove the majority of the white noise for a better extraction of motion features. A zero-velocity detector (reported in [5]) was applied to the averaged data to determine the stance phase during the gait cycle. The results are shown in Fig. 3. On the left are the ZUPT state and the averaged IMU data from the forefoot. On the right of Fig. 3 are the readouts of the IMU located behind the heel. ZUPT state was derived for both mounting positions with the same threshold. For IMUs mounted on the forefoot and behind the heel, Fig. 3 shows an average time duration of the stance phase of 0.498s and 0.363s, and the shock experienced by IMU was on the level of $80 m/s^2$ and $150 m/s^2$, respectively. Both a longer stance phase and a lower level of shock yielded a better navigation accuracy for the IMU mounted on the forefoot. Interruption of the stance phase for the heel showed that the IMU was moving during the stance phase, indicating a less stable stance phase if IMU was mounted behind the heel. One disadvantage of forefoot as the IMU mounting position was that the maximum gyroscope readout was about 800deg/s compared to the 450deg/s if mounted behind the heel. In this study, the gyroscope of IMU had a maximum measuring range of 2000deg/s, and therefore in this case, the higher gyroscope readout was not an issue. However, the choice of an IMU with a sufficient dynamic range is an important consideration for this application.

B. Velocity Uncertainty Determination

To estimate the velocity uncertainty during the stance phase, we first implemented ZUPT-aided inertial navigation algorithm to the IMU data to estimate the trajectory and to extract the stance phases. Next, a free strapdown navigation algorithm was applied to the IMU readouts during the stance phases, assuming a zero initial velocity. The initial orientation of the IMU during the stance phases was obtained from previous navigation results. Velocity propagations during the stance phases are shown in Fig. 4. The average length of the stance phase in this case was around 0.48s, which was comparable to results obtained from the method of averaging. No obvious features could be extracted along the horizontal directions, indicating a random nature of the velocity during the stance

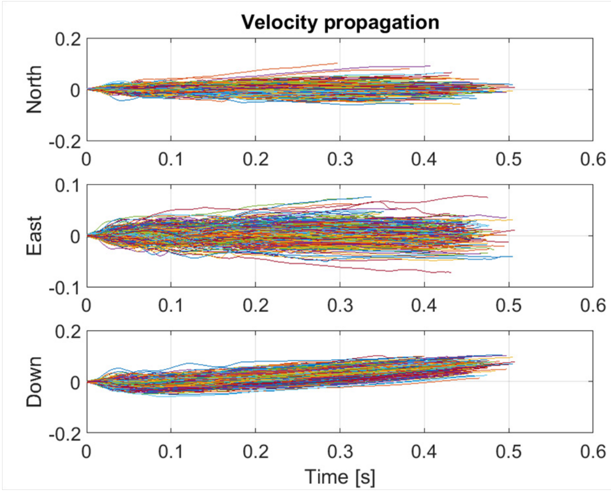

Fig. 4. Velocity propagation along three orthogonal directions during the 600 stance phases.

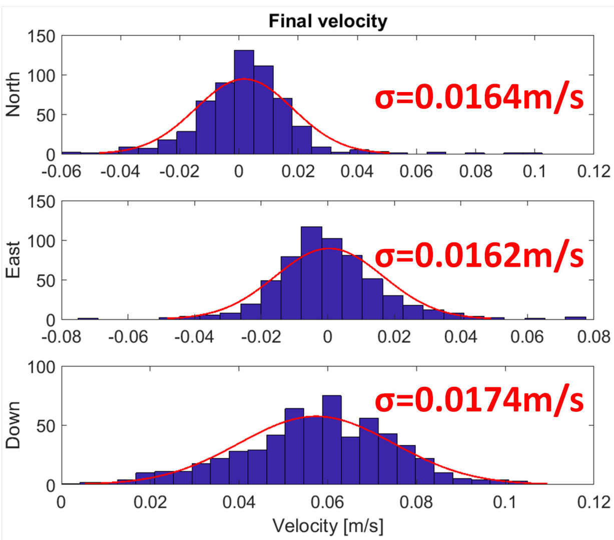

Fig. 5. Distribution of the final velocity along three orthogonal directions during 600 stance phases. Standard deviation is extracted as the average velocity uncertainty during the stance phase.

phase. Finally, distribution of the final velocity was analyzed (Fig. 5) and its standard deviation was calculated to be 0.016m/s and 0.022m/s for IMU mounted on the forefoot and behind the heel, respectively. The standard deviation was set to be the velocity uncertainty during the stance phase. A lower velocity uncertainty for the forefoot showed an advantage of the forefoot as the IMU mounting position. The final velocity distribution was of a bell shape, indicating that it can be approximated as a Gaussian distribution. The velocity bias along the vertical direction might be explained as follows: when the zero-velocity detector determined the start of the stance phase, the foot was not fully stationary and the residual vertical velocity was downward, but the initial velocity of the stance phase was assumed to be zero, and the velocity bias was thereby introduced.

Next, we calculated the velocity uncertainty caused by accelerometer's and gyroscope's white noise [11]:

$$\Delta v_{\text{accel}} = VRW \cdot \sqrt{t} \approx 1 \times 10^{-3} m/s, \qquad (1)$$

TABLE I
STANCE PHASE ANALYSIS SUMMARY WITH DIFFERENT FLOOR TYPES

Floor Type	Step Pace [step/min]	Velocity Uncertainty [m/s]		Stance Phase Length [s]	
		Heel	*Forefoot*	*Heel*	*Forefoot*
Hard Floor	84	0.022	0.016	0.36	0.50
	100	0.025	0.020	0.33	0.39
	112	0.029	0.024	0.29	0.34
Grass Lawn	84	0.046	0.032	0.48	0.55
	100	0.052	0.035	0.38	0.45
	112	0.055	0.045	0.34	0.39
Sand	84	0.060	0.048	0.51	0.48
	100	0.076	0.050	0.37	0.37
	112	0.095	0.051	0.31	0.32

TABLE II
STANCE PHASE ANALYSIS SUMMARY WITH DIFFERENT TRAJECTORIES

Trajectory	Step Pace [step/min]	Velocity Uncertainty [m/s]		Stance Phase Length [s]	
		Heel	*Forefoot*	*Heel*	*Forefoot*
Upstairs	84	0.086	0.042	0.51	0.53
	100	0.088	0.038	0.39	0.45
	112	0.086	0.029	0.33	0.39
Downstairs	84	0.084	0.055	0.48	0.58
	100	0.083	0.042	0.31	0.42
	112	0.080	0.038	0.27	0.30

$$\Delta v_{\text{gyro}} = \sqrt{\frac{1}{3}} ARW \cdot g \cdot t^{3/2} \approx 8 \times 10^{-5} m/s, \qquad (2)$$

where Δv_{accel} is the velocity uncertainty caused by accelerometer's white noise, Δv_{gyro} is the velocity uncertainty caused by gyroscope's white noise, t is the length of the stance phase, and g is the gravity. According to Eqn. (1) and (2), the extracted velocity uncertainty during the stance phase was not related to the IMU noises, since the noise was orders of magnitude lower than what is needed to introduce velocity uncertainty on the order of 0.01m/s.

C. Data Processing Summary

The stance phase analysis with different step paces and floor types is presented in Table I. The velocity uncertainty during the stance phase was highest when walking on the sand, then on the grass lawn, and it was lowest when walking on the hard floor. This result was expected. The same conclusion was drawn in all nine scenarios that the forefoot was a better IMU mounting position than the heel with an average of 20% lower velocity uncertainty and about 20% longer stance phase period.

Table II lists the analysis of walking upstairs and downstairs, while Table III lists the analysis of walking on hard floor by different persons (different walking patterns). A similar result was obtained for all cases, concluding that a longer stance phase and a lower velocity uncertainty should be expected to be achieved with IMU mounted on the forefoot.

IV. EXPERIMENTAL VERIFICATION

In previous sections, the forefoot and the heel were compared as candidates for IMU mounting positions in terms of parameters related to navigation accuracy. In this section, a

TABLE III
STANCE PHASE ANALYSIS SUMMARY WITH DIFFERENT PERSONS

Floor Type	Step Pace [step/min]	Velocity Uncertainty [m/s]		Stance Phase Length [s]	
		Heel	*Forefoot*	*Heel*	*Forefoot*
Agent 1	84	0.022	0.016	0.36	0.50
	100	0.025	0.020	0.33	0.39
	112	0.029	0.024	0.29	0.34
Agent 2	84	0.044	0.028	0.49	0.50
	100	0.040	0.026	0.29	0.31
	112	0.034	0.020	0.27	0.27
Agent 3	84	0.052	0.035	0.48	0.52
	100	0.071	0.026	0.34	0.37
	112	0.022	0.020	0.28	0.30
Agent 4	84	0.029	0.026	0.38	0.42
	100	0.040	0.034	0.28	0.33
	112	0.031	0.021	0.27	0.28

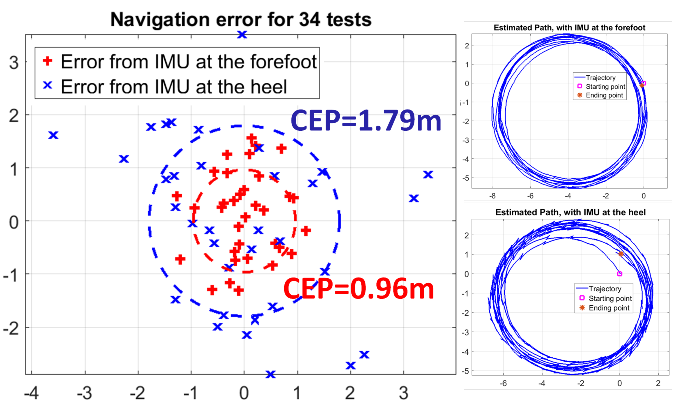

Fig. 6. On the left is the navigation error of 34 tests of the same circular trajectory. On the right are typical estimated trajectories from the IMU on the forefoot (upper) and behind the heel (lower).

direct correlation between the IMU mounting position and the navigation accuracy is presented.

A circular path with a diameter of 8m and 10 laps was used as a trajectory to experimentally demonstrate the effect of IMU mounting position on the CEP. The starting point and the end point of the trajectory were the same, so that any difference between the two points in the estimation would be counted as the navigation error. 34 tests were recorded with an average navigation time of 260s, and the navigation errors for all tests are presented in Fig. 6. The CEP was reduced from 1.79m to 0.96m with the same IMU, but mounted on the forefoot instead of behind the heel. On the right side of Fig. 6 are two estimated trajectories with data from the forefoot (upper) and the heel (lower). The smoothness of the trajectory and the final navigation error were both better for IMU mounted at the forefoot.

A longer trajectory was tested with a navigation time of 15 minutes. The result is shown in Fig. 7. A much smaller navigation error was achieved with IMU mounted on the forefoot than behind the heel. An advantage of the IMU placement on the forefoot was thus demonstrated experimentally.

V. CONCLUSIONS

The forefoot was proven to be a more preferable IMU mounting position than the heel in the ZUPT-aided pedestrian

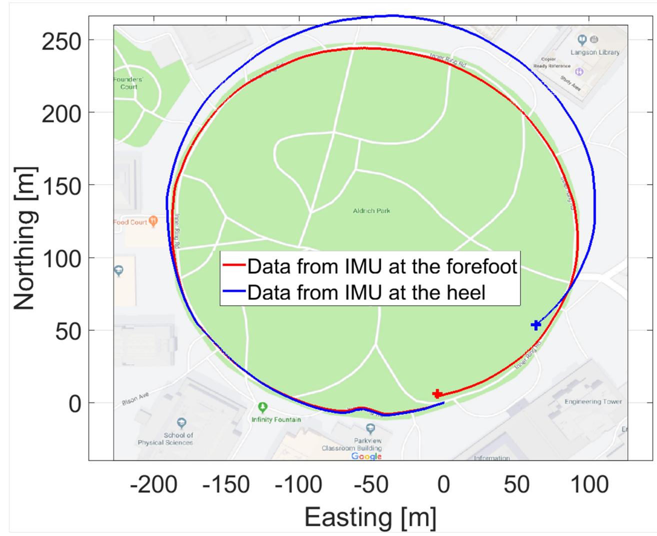

Fig. 7. Results of the field test with IMUs mounted on the forefoot and behind the heel.

inertial navigation due to a longer stance phase, lower shock level and a lower velocity uncertainty during the stance phase. A direct correlation between the IMU mounting position and the navigation error was established. To the best of our knowledge, a technique to extract the velocity uncertainty during the stance phase was developed and demonstrated for the first time.

REFERENCES

[1] X. Yun, E. R. Bachmann, H. Moore, and J. Calusdian, “Self-contained position tracking of human movement using small inertial/magnetic sensor modules.” IEEE International Conference on Robotics and Automation, Apr. 10-14, 2007, Roma, Italy, pp. 2526-2533.

[2] M. Ma, Q. Song, Y. Li, and Z. Zhou, “A zero velocity intervals detection algorithm based on sensor fusion for indoor pedestrian navigation.” IEEE Information Technology, Networking, Electronic and Automation Control Conference (ITNEC), Dec. 15-17, 2017, Chengdu, China, pp. 418-423.

[3] E. Foxlin, “Pedestrian tracking with shoe-mounted inertial sensors,” *IEEE Computer Graphics and Applications*, 25, (6), pp. 38-46, 2005.

[4] Y. Wang, D. Vatanparvar, A. Chernyshoff, and A. M. Shkel, “Analytical Closed-Form Estimation of Position Error on ZUPT-Augmented Pedestrian Inertial Navigation.” *IEEE Sensors Letters*, 2, (4), pp. 1-4, 2018.

[5] Y. Wang, A. Chernyshoff, and A. M. Shkel, “Error analysis of ZUPT-aided pedestrian inertial navigation.” *IEEE Intl. Conf. on Indoor Positioning and Indoor Navigation (IPIN)*, Nantes, France, Sep. 24-27, 2018, pp. 206-212.

[6] J. O. Nilsson, A. K. Gupta, and P. Handel, “Foot-mounted inertial navigation made easy.” *International Conference on Indoor Positioning and Indoor Navigation (IPIN)*, Oct. 27-30, 2014, Busan, Korea, pp. 24-29.

[7] M. Laverne, et al., “Experimental validation of foot to foot range measurements in pedestrian tracking.” *ION GNSS Conference*, Portland, OR, USA, Sep. 19-23, 2011, pp. 1386-1393.

[8] M. Ren, K. Pan, Y. Liu, H. Guo, X. Zhang, and P. Wang, “A novel pedestrian navigation algorithm for a foot-mounted inertial-sensor-based system,” *Sensors*, vol. 16, no. 1, pp.139, 2016.

[9] I. Skog, J. O. Nilsson, and P. Handel, “Evaluation of zero-velocity detectors for foot-mounted inertial navigation systems.” *IEEE International Conference on In Indoor Positioning and Indoor Navigation (IPIN)*, Sept 15-17, 2010, Zurich, Switzerland, pp. 1-6.

[10] VectorNav VN-200 GPS-Aided Inertial Navigation System Product Brief. https://www.vectornav.com/docs/default-source/documentation/vn-200-documentation/PB-12-0003.pdf?sfvrsn=749ee6b9_13

[11] O. J. Woodman, *An Introduction to Inertial Navigation* (No. UCAM-CL-TR-696). University of Cambridge, Computer Laboratory, 2007.